γ-Sarcoglycan deficiency increases cell contractility, apoptosis and MAPK pathway activation but does not affect adhesion

Maureen A. Griffin[1,2], Huisheng Feng[1,3], Manorama Tewari[1,2], Pedro Acosta[1,3], Masataka Kawana[1,3], H. Lee Sweeney[1,3,4] and Dennis E. Discher[1,2,4,*]

[1]Pennsylvania Muscle Institute, University of Pennsylvania Medical Center, D-700 Richards Building, 3700 Hamilton Walk, Philadelphia, PA 19104-6083, USA
[2]Department of Chemical and Biomolecular Engineering, Towne Building, 220 South 33rd Street, University of Pennsylvania, Philadelphia, PA 19104-6393, USA
[3]Department of Physiology, University of Pennsylvania Medical Center, 3700 Hamilton Walk, Philadelphia, PA 19104-6085, USA
[4]Graduate Group in Cell and Molecular Biology, University of Pennsylvania Medical Center, 3620 Hamilton Walk, Philadelphia, PA 19104-6058, USA
*Author for correspondence (e-mail: discher@seas.upenn.edu)

Accepted 10 January 2005
Journal of Cell Science 118, 1405-1416 Published by The Company of Biologists 2005
doi:10.1242/jcs.01717

Summary

The functions of γ-sarcoglycan (γSG) in normal myotubes are largely unknown, however γSG is known to assemble into a key membrane complex with dystroglycan and its deficiency is one known cause of limb-girdle muscular dystrophy. Previous findings of apoptosis from γSG-deficient mice are extended here to cell culture where apoptosis is seen to increase more than tenfold in γSG-deficient myotubes compared with normal cells. The deficient myotubes also exhibit an increased contractile prestress that results in greater shortening and widening when the cells are either lightly detached or self-detached. However, micropipette-forced peeling of single myotubes revealed no significant difference in cell adhesion. Consistent with a more contractile phenotype, acto-myosin striations were more prominent in γSG-deficient myotubes than in normal cells. An initial phosphoscreen of more than 12 signaling proteins revealed a number of differences between normal and γSG$^{-/-}$ muscle, both before and after stretching. MAPK-pathway proteins displayed the largest changes in activation, although significant phosphorylation also appeared for other proteins linked to hypertension. We conclude that γSG normally moderates contractile prestress in skeletal muscle, and we propose a role for γSG in membrane-based signaling of the effects of prestress and sarcomerogenesis.

Key words: Sarcoglycan, Muscular dystrophy, Limb-girdle muscular dystrophy, Differentiation

Introduction

Of nine diagnosed phenotypes of muscular dystrophy (MD), most result from a disruption in the dystrophin-associated membrane proteins known as the dystrophin glycoprotein complex (DGC). One component of the DGC is γ-sarcoglycan (γSG) whose absence leads to a particular form of MD, referred to as limb-girdle MD2C (LGMD2C) (Noguchi et al., 1995; Bushby, 1999). The DGC colocalizes with integrins and other adhesion proteins at the sarcolemma (Lakonishok et al., 1992; Paul et al., 2002), motivating studies of whether the components of the DGC contribute to adhesion and integrity of skeletal muscle (Kaariainen et al., 2000; Kramarcy and Sealock, 1990). Sarcoglycans have been shown to colocalize specifically with focal adhesion proteins (Yoshida et al., 1998) and a loss of α-sarcoglycan inhibits cell adhesion to collagen substrates (Yoshida et al., 1996). Nevertheless, little is directly known of the normal role of γSG in adhesion, signaling or contractility.

As dystrophin and the DGC contribute to the tensile strength of muscle as well as membrane integrity and elasticity (Bradley and Fulthorpe, 1978; Grady et al., 1997; Straub et al., 1997), γSG was initially expected to also play a role in the strength and integrity of the sarcolemma. In work with muscle from knockout mice however, no decrease in tensile strength or membrane integrity was found in γSG-deficient muscle compared with normal muscle. Apoptosis is reported to increase (Hack et al., 1998), but the underlying mechanism for the MD phenotype is unclear.

A possible role for γSG in adhesion, and perhaps anchorage-dependent signaling, is suggested by integration of γSG into the DGC and adhesion complexes, however, connections to cytoskeletal processes are also possible. Membrane adhesion complexes generally mediate a balance between cytoskeletal tension, contractility, or 'prestress' and a mechanical resistance of extracellular substrates or matrix (ECM) (Lee et al., 1998; Stamenovic et al., 2002). Prestress has been measured for many cell types under various conditions (Hubmayr et al., 1996; Potard et al., 1997; Wang et al., 1993; Wang et al., 2002), and various components of the cytoskeleton have been individually associated with this prestress, including actin, myosin, microtubules, and intermediate filaments. Signaling aspects of such sustained contractility are unclear, especially in relation to γSG function.

We provide initial evidence here of signaling pathways that are perturbed in γSG$^{-/-}$ muscle. First, however, we used novel micromanipulation techniques to examine the prestress and adhesion dynamics of both normal and γSG$^{-/-}$ myotubes. In decoupling the effects of adhesion from the effects of cellular prestress, we found that γSG$^{-/-}$ cells have similar adhesive properties to normal cells, but they appear to have enhanced prestress associated with contractility. This seems to be moderated in its effects by downregulation of apoptotic signals that contribute to the MD phenotype. The results here may suggest new approaches to influence the course of disease.

Materials and Methods

Cell culture

Primary skeletal myoblasts were harvested from 1-day-old mice as previously described (Neville et al., 1998). Both normal (C57) and homozygous knockout mice for γ-sarcoglycan (γSG$^{-/-}$) (Hack et al., 1998) were used. After harvesting, ~10^5 cells were plated onto either collagen-coated Aclar (Ted Pella, Redding, CA) or interpenetrating network (IPN)-patterned glass. Cultures were maintained in DMEM (Gibco Laboratories, Grand Island, New York) supplemented with 22% horse serum (Gibco), 8% embryo extract (US Biological, Swampscott, MA), 1% L-glutamine (Gibco) and 1% penicillin/streptomycin at 10,000 U/ml and 10,000 μg/ml, respectively (Gibco). Medium was changed every other day.

Microscopy

All microscopy was done with a Nikon TE300 inverted microscope. Fluorescently labeled cells and/or nuclei were imaged with either a 40× 0.45 NA objective (TUNEL assays) or a 60× 1.45 NA oil objective (immunofluorescence). Images were recorded with a Cascade CCD camera (Photometrics, Tucson, AZ), and fluorescence intensity was measured using Scion Image (Scion Corporation, Frederick, MD). Relaxing or peeling of cells were observed through a 10× 0.17 NA phase-contrast objective and images were recorded onto video through a video-rate camera (model JE8242, Javelin Systems, Torrance, CA).

TUNEL assay

TUNEL assays were performed on formaldehyde-fixed samples using the ApopTag in situ apoptosis fluorescein detection kit (Chemicon International, Temecula, CA).

Fluorescence staining

Both C57 and γSG$^{-/-}$ cells were stained for actin, myosin, α-sarcoglycan (αSG) and γSG. Cells were rinsed with PBS and fixed in 10% formaldehyde. Cells were then permeabilized in 0.1% Triton X-100 and incubated in a 5% bovine serum albumin blocking solution at 37°C for 1 hour. After blocking, the cells were incubated overnight at 4°C in one of the following four primary antibody solutions in PBS: 1:50 mouse anti-myosin (Zymed, San Francisco, CA, 18-0105), 1:10 mouse anti-utrophin (NovoCastra, Newcastle-upon-Tyne, UK, NCL-DRP2), 1:100 mouse anti-αSG (NovoCastra, NCL-a-SARC), or 1:100 mouse anti-γSG (NovoCastra, NCL-g-SARC). Control samples were incubated in pure PBS without primary antibody. Cells were then fluorescently labeled by incubation for 1 hour at 37°C in 1:100 FITC-conjugated anti-mouse IgG (F2761; Molecular Probes, Eugene, OR) in PBS. Cells previously labeled for myosin were co-labeled for actin at this point by adding 60 μg/ml TRITC-phalloidin (Sigma) to the secondary antibody solution. Finally, the cell nuclei were labeled with 1:100 Hoechst 33342 (Molecular Probes), and the samples were mounted onto slides using Gel/Mount (Biomedia, Foster City, CA).

For quantification of fluorescence, a relative intensity *RI* was defined. As *RI*=1 means there is no increase in fluorescence over the control, the *RI*s are represented with a minus sign for $RI \leqslant 1$ and a single plus sign for $1<RI \leqslant 1.5$. An additional plus sign is added for every 0.5 increase after 1.5, so an *RI* of 2.7, for example, is represented as '+++'.

Single cell relaxation

Patterned myotubes were allowed to relax as previously described (Griffin et al., 2004a). In brief, one end of an isolated myotube was mechanically detached from the substrate with a micropipette pre-incubated in BSA. The myotube then recoiled or relaxed for up to 6 minutes. The relative length of the myotube during the process was monitored by video, and at times, the stage was repositioned in order to keep the cell in the field of view.

Single cell peeling

Isolated myotubes were also forcibly peeled from the substrate using the micropipette peeling technique described (Griffin et al., 2004a). Briefly, a large-bore micropipette with an inner diameter of 75 μm (Polymicro Technologies, Phoenix, AZ) was pre-incubated in BSA to minimize cell-pipette interactions. The pipette was attached to a syringe pump (model SP120p-300, World Precision Instruments, Sarasota, FL) with a flow rate that ranges from 0.001 μl/minute to 602 μl/minute. After one end of the cell was mechanically detached, the syringe pump was used to initiate a flow and cells were peeled from the substrate using a motorized stage. Because of the large size of the micropipette compared with the dimensions of the cell, the shear stress, τ_{cell} of the aspirating fluid drove the cell peeling, and the peeling tension T_{peel} is simply the integral of τ_{cell} over the length of cell inside the pipette, L_{asp}. Peeling experiments were recorded in the same manner as relaxation experiments, and the velocity of the peel, V_{peel}, was measured as a function of T_{peel}.

Phosphoscreen on TA muscle

Whole cell lysates were prepared from samples of unstretched and stretched TA (tibialis anterior) muscle obtained from juvenile (8-week-old) C57 and γSG$^{-/-}$ mice according to published protocols (Pelech et al., 2003). Stretching of ~10% for 20 minutes was done after dripping calcium-free PBS on the muscle. 300 μg of these protein lysates were separated by SDS-PAGE and were immunoblotted in a 20-lane Immunetics multiblotter using commercially available antibodies as recently described for the Kinexus KPSS5.0-phospho and KPSP-1 phosphoscreen (Pelech et al., 2003). The immunoblots were then subjected to enhanced chemiluminescence, and were identified based upon human protein sequences. Finally, the bands were detected with a Bio-Rad FluorS Max Multi-imager (Bio-Rad Laboratories, Hercules, CA) and the relative intensities were quantified with Quantity One software (Bio-Rad) and reported as arbitrary units (a.u.), normalized to correct for differences in protein concentration. The results are accurate to within 25%.

Results

Apoptosis is increased in γSG$^{-/-}$ cells

As in human patients, muscle in γSG$^{-/-}$ mice develops significant fibrosis, particularly in the heart (Hack et al., 1998). Fibrosis stiffens tissue, and this stiffness was emulated here by growing cells on a rigid glass substrate (with a pre-adsorbed collagen monolayer for adhesion). For comparison, cells were also grown on a thick and soft collagen film on Aclar, serving as a control substrate for TUNEL staining of cells. The extent

of apoptosis was quantified by calculating the ratio of TUNEL fluorescence intensities for nuclei in cells grown on glass (NI_{glass}) to the intensities for nuclei in cells grown on Aclar (NI_{Aclar}).

NI_{glass}/NI_{Aclar} was determined for C57 and γSG$^{-/-}$ cells at both 2 and 7 days after plating (Fig. 1). In comparing day 7 to day 2, we found a 17-fold increase in the NI_{glass}/NI_{Aclar} for γSG$^{-/-}$ cells. The ratios for C57 cells at both days were not significantly different, and also compared well with the NI_{glass}/NI_{Aclar} for γSG$^{-/-}$ cells at day 2. Thus, we concluded that within 7 days, γSG$^{-/-}$ cells cultured on glass apoptosed to a far greater extent than either C57 cells or nascent γSG$^{-/-}$ myotubes.

γSG$^{-/-}$cells striate more than controls

Representative proteins expressed by C57 and γSG$^{-/-}$ cells on day 6 in culture were quantified as the average fluorescence intensity after immunostaining of parallel cultures. Intensities were measured for cells growing both on top of other cells (upper layer) and also directly on the IPN-patterned glass (lower layer). The cells-on-cells accounted for approximately 60% of the patterned cells and occurred as cells crawled onto other cells, without any outside impetus. Intensities were normalized by dividing by the average intensity of cells stained only with secondary, and not primary, antibody. The resulting values were defined as the relative intensities and converted to simpler '+' and '–' notation in Table 1 (see Materials and Methods).

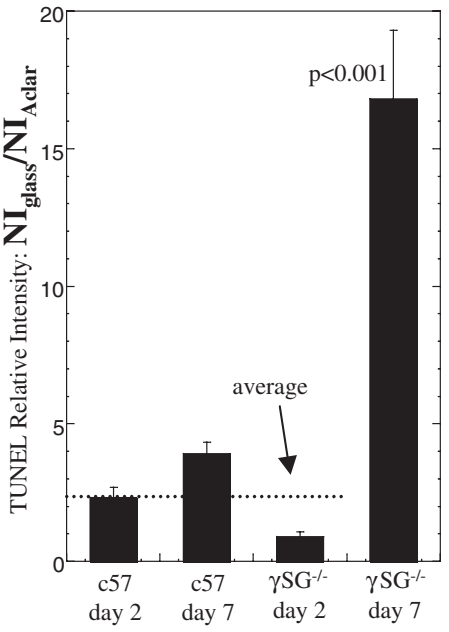

Fig. 1. Apoptosis of primary cells. γSG-deficient myotubes on rigid substrate exhibited greater apoptosis than wild-type C57 myotubes at day 7. Both C57 and γSG$^{-/-}$ cells were split, plated in parallel on soft collagen-substrates or rigid IPN-patterned coverslips, and later tested for apoptosis by TUNEL assay at day 2 and day 7. The mean intensity of nuclei for the cells on coverslips was divided by the mean intensity for the cells grown on the collagen-substrates for each day. Error bars represent the s.e.m. of the intensities of at least 50 cells. The relative intensity for γSG$^{-/-}$ at day 7 was significantly greater (17-fold) (P<0.001) than the relative intensity at day 2, indicating that γSG$^{-/-}$ cells cultured on rigid substrate apoptosed to a far greater extent than normal cells under normal conditions.

Table 1. Protein expression of cells on IPN-patterned glass

	C57		γSG$^{-/-}$	
	Lower layer	Upper layer	Lower layer	Upper layer
γSG	+++	+++	–	–
αSG	+	+	–	+
Myosin	+	+++	–	++
Utrophin	+++	+++++	+	+

Table 1 confirms that the γSG$^{-/-}$ cells did not express γSG and also lost αSG (Hack et al., 1998). We also saw that both cell types growing directly on the IPN-patterned glass expressed significantly less myosin than cells growing on top of other cells at day 6. At day 6, utrophin followed a similar trend; γSG$^{-/-}$ cells showed less utrophin than normal cells and C57 cells-on-cells expressed slightly more utrophin than cells-on-glass. As it has been documented that utrophin expression in muscle culture increases and then decreases with differentiation (Radojevic et al., 2000), the reduced utrophin levels implied that γSG$^{-/-}$ cells were either less differentiated or more differentiated than normal cells. Results below show that the latter appeared to be the case.

In addition to measuring the fluorescence intensity, cells immunostained for myosin were scored based on the amount of structured or striated myosin present (Fig. 2). Structured myosin was identified as fibrous and non-diffuse, but without any striations. Although a small percentage of cells growing directly on the glass formed myosin fibers instead of exhibiting only diffuse myosin (Fig. 2B), completely striated myosin formed only in cells-on-cells (Fig. 2C), consistent with results previously reported by our laboratory (Engler et al., 2004a; Engler et al., 2004b; Griffin et al., 2004b). Striated myosin was seen in almost 50% of γSG$^{-/-}$ cells-on-cells, whereas in normal, C57 cells, less than half that amount of striation was observed (Fig. 2D).

Although the upper layer of C57 cells seemed to express more myosin than the upper layer of γSG$^{-/-}$ cells (Table 1), the myosin in γSG$^{-/-}$ cells showed more structure and striation overall. It could be that the tighter organization made immunostaining less efficient, reducing the intensity. Regardless, the data in Table 1 indicated differences between upper and lower cells.

γSG$^{-/-}$ cells relax more than controls

By detaching the end of an adherent myotube from its substrate, the relative length of the myotube was seen to decrease as the cell relaxed from its adhesive constraints (Fig. 3A). The decay was exponential over time (Fig. 3B). Myotube relaxation can be modeled simply as a Voigt solid (Griffin et al., 2004a), and the relative length fits very well to the equation,

$$L / L_{init} = 1 - A\,(1 - e^{-t/\tau}),$$

where L is the cell length, L_{init} is the initial length, A is the shortening amplitude, and τ is the characteristic time. Data for 10-15 cells of each type (all relaxed at day 6) were binned by time, averaged, and compared in Fig. 3B.

Although γSG$^{-/-}$ cells exhibited more heterogeneity during relaxation, there was a clear difference in relaxation dynamics

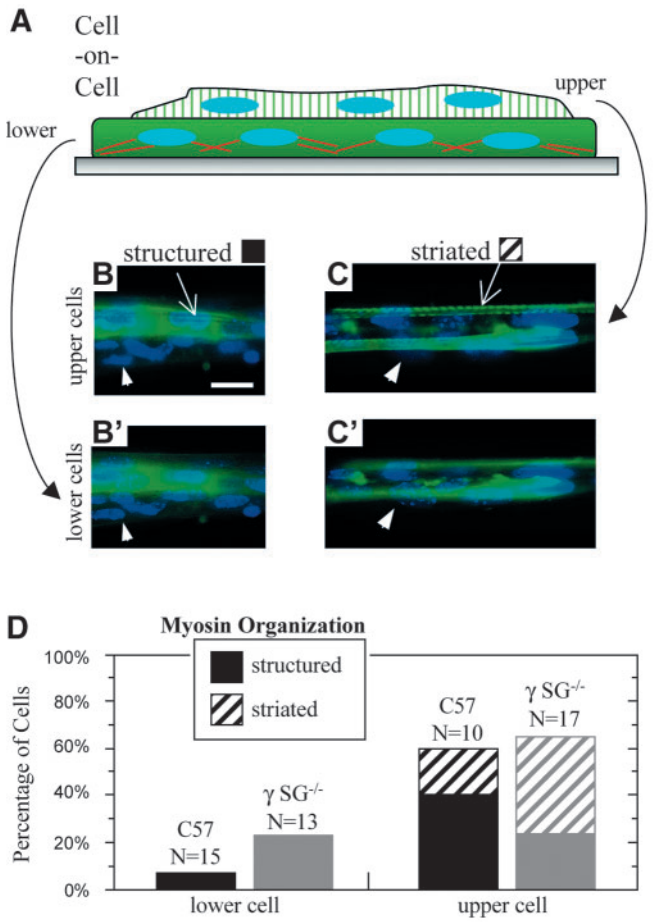

Fig. 2. Myosin expression and striation in primary cells. A fraction of primary cells crawled on top of other cells while in culture. (A) A sketch of the two-cell system indicating that only the upper cell was striated. (B,C) Two different fields with γSG$^{-/-}$ cells growing on top of other cells. The upper layer of cells is in focus in (B,C) and the lower layer of cells is in focus in (B′,C′). There is ~6 μm height difference between the two focal planes. The arrowheads point to nuclei that are in focus in the lower layer. Myosin appeared highly expressed and often exhibited some structure (B) or complete striation (C) only in cells growing on top of other cells. The arrow in B indicates a fiber of structured myosin in the myotube and the arrow in C indicates a fully striated myofiber. (D) Almost twice as many γSG$^{-/-}$ cells were striated as C57 cells. For both cell types, only the upper cell was striated. Bar, 20 μm.

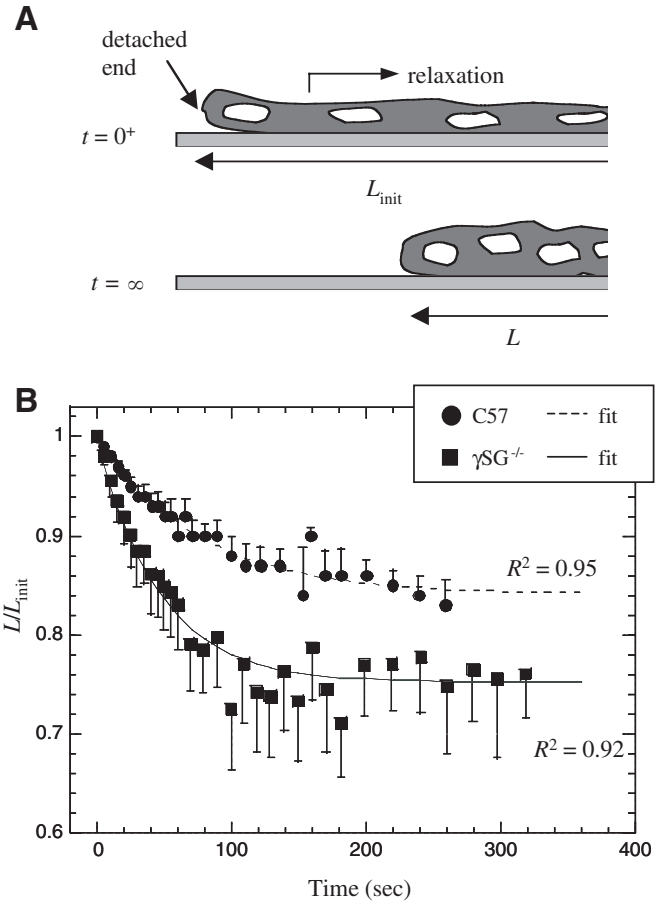

Fig. 3. Relaxation dynamics of normal and γSG-deficient myotubes.(A) Length relaxation, or self-peeling, occurred when one end of the cell was mechanically detached with a micropipette at t=0. (B) Data for 6-day-old C57 (15 cells) and γSG$^{-/-}$ (10 cells) were binned by time, averaged, and fit by $L/L_{init} = 1 - A\,(1 - e^{-t/\tau})$ with the indicated R^2 values. Based on the fit of the binned data, A_{C57}=0.16 and $A_{\gamma SG}$=0.31. Error bars represent the s.e. of the binned means. Although γSG$^{-/-}$ cells relaxed faster and to a greater extent than C57 cells, γSG$^{-/-}$ cells showed more heterogeneity.

compared with normal C57 cells. The average shortening amplitude of γSG$^{-/-}$ cells was twice as large as that of C57 cells. This difference applied regardless of whether A was calculated from a fit of the data compiled from multiple cells as in Fig. 3B, or by averaging A from fits of individual cells. There was no significant difference in time constants between the cell types. Because τ is indicative of the adhesive drag, whereas A represents the cellular prestress, the stronger dependence on A suggested that a contractile prestress, rather than adhesion, caused the difference in relaxation dynamics.

When observing fixed cells that have not been mechanically disturbed, we also saw that a fraction of isolated myotubes growing on IPN-patterned glass appeared very wide in the center compared with the ends (Fig. 4A). This shape was reminiscent of a cell mechanically induced to relax by micropipette perturbation: in either case the cell is tethered at one end, but it shortens and widens as it pulls back. It appeared that cells with this wider shape were ‘self-relaxing’ or relaxing without mechanical end-detachment. The percentage of cells undergoing self-relaxation was quantified by determining the ratio of cell widths at the middle (W_{mid}) compared with the width at the end (W_{end}) (Fig. 4B). Based on these data, we concluded that more γSG$^{-/-}$ cells than C57 cells were sufficiently stressed to self-relax. Cells of a rectangular shape were studied further in their adhesion to determine whether adhesion of γSG$^{-/-}$ cells was reduced or intracellular stresses were higher compared with normal cells.

γSG$^{-/-}$cells and controls show similar adhesion

Two parameters control the relaxation process: cellular prestress, which drives cell relaxation, and drag, which slows

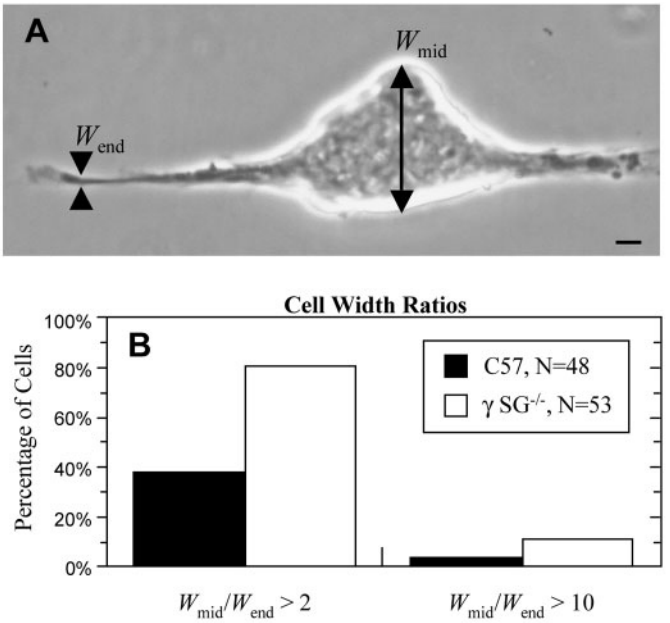

Fig. 4. Cell width ratios. (A) The mid-width of cells W_{mid} was compared with the width near the end W_{end}. (B) Twice as many γSG$^{-/-}$ cells had a high width ratio as C57 cells. Bar, 20 μm.

relaxation dynamics. C57 cells therefore either have less initial prestress than γSG$^{-/-}$ cells, or more drag, or a combination of both. In order to further separate the effects of prestress from the effects of adhesive drag, especially relevant because γSG is a membrane-localized protein, cells were forcibly peeled from the substrate using the micropipette technique described in the Materials and Methods and depicted in Fig. 5A. This technique quantified the adhesion strength of cells, and isolated the adhesive effect from the prestress. Peeling, like relaxation, was conducted on 6-day-old cells.

A typical example of the peeling velocity (V_{peel}) versus imposed tension (T_{peel}) for a single peeling run is plotted in Fig. 5B. The velocity of a peeling primary cell fluctuated during the course of the peel owing to strongly adherent points along the cell length. Such strongly adherent points were seen in previous studies and defined as physical focal adhesions (PFAs) (Griffin et al., 2004a) (Fig. 5B, squares). For both normal C57 and γSG$^{-/-}$ cells, peak velocities, V_{peel_pk} versus T_{peel} were binned according to the tension and averaged (Fig. 5C), and the results were then fitted to the equation,

$$V_{peel\_pk} = a \ln (T_{peel}) + b.$$

As is clear from Fig. 5C, there was no significant difference between the peeling fits for the two cell types. The intercept $T_o = e^{(-b/a)}$ represents the minimum tension required to detach a cell from the substrate. Recent studies of myotubes adhering to different substrates have demonstrated considerable

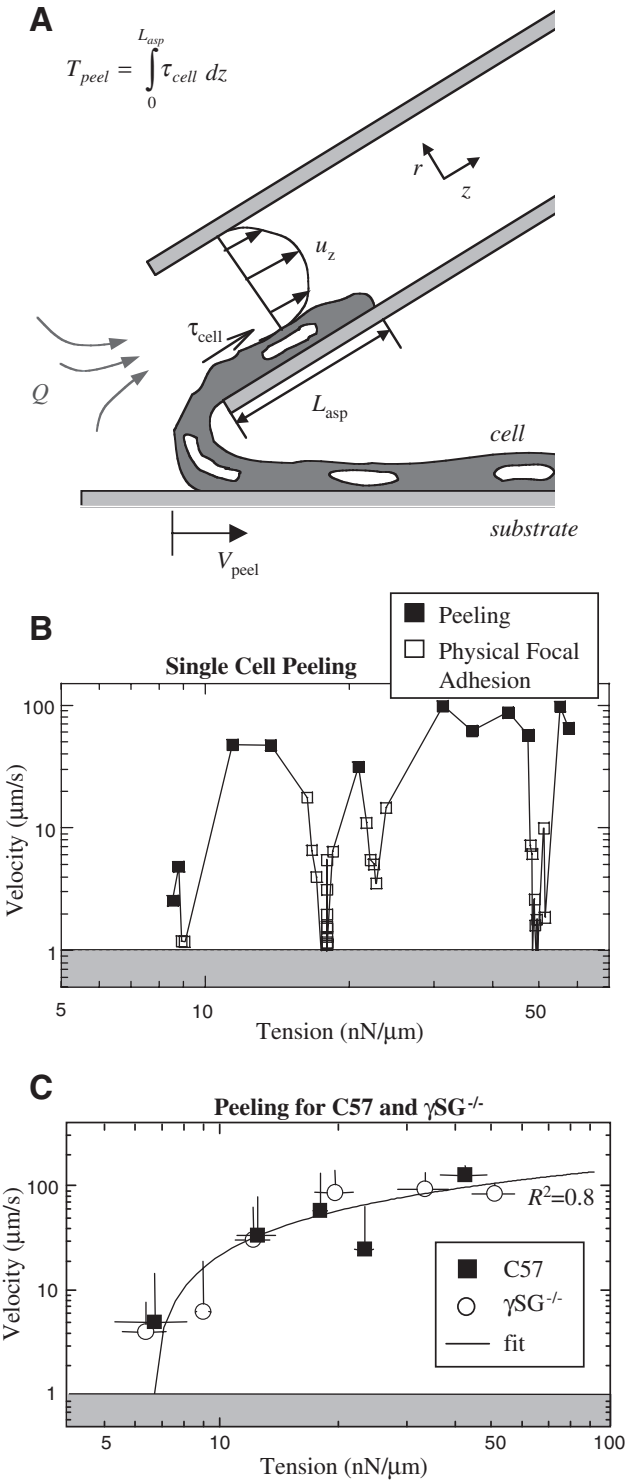

Fig. 5. Dynamic adhesive strength of primary myotubes. C57 and γSG$^{-/-}$ myotubes have similar dynamic adhesive strength. (A) Forced peeling was done with a large-bore micropipette. The shear stress, τ_{cell}, of the aspirating fluid imposed a tension, T_{peel}, which peeled the cell from the substrate at a velocity V_{peel}. The flow rate, Q, was held constant by a syringe pump, but T_{peel} increased linearly with the length of cell inside the micropipette, L_{asp}. The fluid velocity u_z within the pipette is parabolic in profile as sketched. (B) A typical peeling run exhibits dips in the velocity as a function of tension. These dips correspond to physical focal adhesions (PFA, empty squares) along the length of the cell. The velocity envelope that defines 'peeling' (filled squares) can be compared between cell types. (C) A comparison of peeling data for normal (C57) and γSG$^{-/-}$ cells revealed no significant difference in peeling dynamics. The R^2 for the C57 and γSG$^{-/-}$ fits are 0.71 and 0.84, respectively.

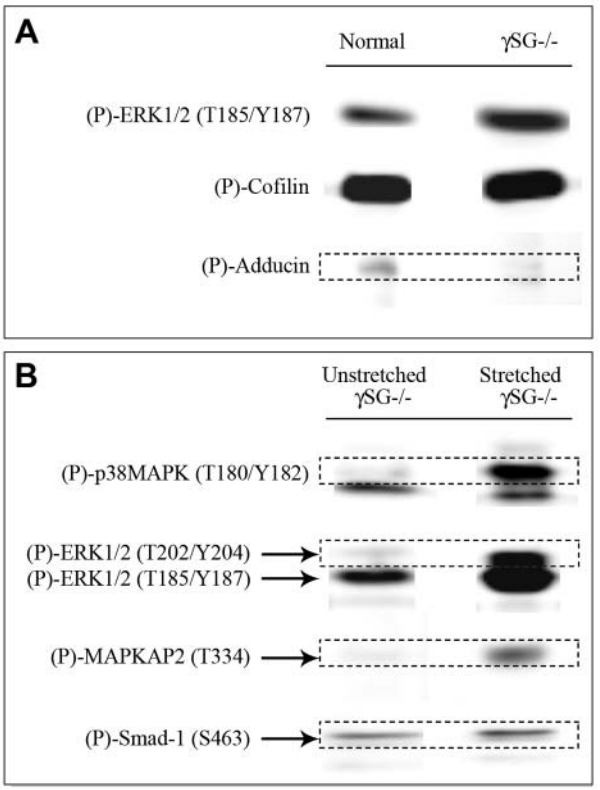

Fig. 6. Phosphoprotein comparisons of normal and γSG-deficient TA muscle. (A) Immunoblots of tissue lysates show significant activation of ERK-1 and downregulation of adducin-γ phosphorylation with no changes in cofilin in $\gamma SG^{-/-}$ tissue compared with control tissue. (B) Blots of stretched and unstretched $\gamma SG^{-/-}$ tissue show hyperactivation of p38 MAPK, ERK1/2, MAPKAP2 and Smad1 in stretched tissue.

differences in T_o and so the method appears sufficiently sensitive (Engler et al., 2004b). Here, however, for both normal C57 and $\gamma SG^{-/-}$ myotubes, this peeling tension is T_o=6 nN/μm. This result was obtained regardless of whether T_o was calculated by averaging the individual intercepts for the separate fits, or determined directly from fitting both sets of data at once.

ERK-1, MAPKAPK2 and MYPT1/2 hyperactivation in $\gamma SG^{-/-}$ cells

Apoptosis seen here and in vivo (Hack et al., 1999) in $\gamma SG^{-/-}$ myocytes as well as the hypercontractility described above suggest possible changes in signaling pathways. Our initial phosphoscreens here are focused on activators, especially the MAP kinases ERK and p38-MAPK, which are midstream in signaling pathways. More than a dozen phosphoproteins in $\gamma SG^{-/-}$and normal TA muscle were quantified (Fig. 6 and Table 2). Although a screen of the cultured myotubes would also have been desirable, protein yields from the micropatterns were far too limited.

At least four phosphoproteins appear hyperactivated in $\gamma SG^{-/-}$ muscle relative to constitutive levels in normal muscle: (P)-ERK1, (P)-MAPKAPK2, (P)-MYPT1/2, and (P)-FAK. ERK1 showed the greatest hyperactivation (+126%), at more than twofold above normal (Table 2). As discussed below, hyperactivation of ERK in these non-proliferating, terminally differentiated cells appears consistent with apoptotic mechanisms.

(P)-hsp27 appeared weakly activated in $\gamma SG^{-/-}$ muscle but not detectably phosphorylated in normal muscle (data not shown). Eight other proteins examined showed no significant difference between normal and $\gamma SG^{-/-}$ tissue. This included the focal adhesion protein paxillin and the most strongly reactive phospho-species detected, (P)-cofilin, which is involved in actin cytoskeleton reorganization in crawling cells. Table 2 indicates that at least six phosphoproteins showed decreased activation in $\gamma SG^{-/-}$ muscle: (P)-adducin-γ, (P)-MAPKAP2 (at T334), (P)-p38MAPK, (P)-SMAD-1, (P)-adducin-α and (P)-AcCoA-Carb. Note that the adducins are also involved in actin cytoskeleton reorganization and showed highly significant changes relative to normal tissue whereas (P)-cofilin did not. Also, the midstream signaling molecules like p38 MAPK and MAPKAP2 showed significantly lower phosphorylation indicating phospho-site-specific functions. These differences between muscle samples, with both up- and downactivation, are discussed later.

Hyperphosphorylation in stretched TA muscles

Given the in vitro and in vivo stress/apoptosis demonstrations of $\gamma SG^{-/-}$ tissue, we focused here more on the upstream or midstream effectors rather than on downstream markers of mechanotransduction. A select set of 18 selected phosphoproteins were compared for stretch activation in normal and $\gamma SG^{-/-}$ muscle. As shown in Fig. 6 and Table 3 hyperactivation of ERK1/2 was more than several-fold above basal levels in both normal and $\gamma SG^{-/-}$ stretched muscles. P38 MAPK and MAPKAPK2 activation exhibited the most striking changes in stretched muscles, indicating a p38 MAPK pathway in stretch-induced mechanotransduction. Importantly, the focal adhesion phosphoproteins paxillin and FAK did not show any significant change between stretched and unstretched tissue, however, and the activation of the regulatory factor Smad1 was only slightly higher in $\gamma SG^{-/-}$ stretched muscle. Smad1 is known to mediate extracellular signaling, transferring mechanical strains into transcriptional events (Scherer and Graff, 2000).

Apoptosis/survival phosphoproteins in muscle tissues of normal and $\gamma SG^{-/-}$

Based on our in vitro studies of apoptosis, we also included upstream ‘apoptotic’ proteins in the initial phosphoscreen. As shown, in Table 2, (P)-ERK, and (P)-FAK were activated and have been shown to be regulators of cell apoptosis/survival. FAK activation at two different tyrosine residues Y577 and Y397 proves to be similarly hyperactivated (+114 and +38%) giving values above the accepted limits of significance (>25%). PKC-α, PKC-ε the signaling molecules and CREB, a transcriptional regulatory protein, showed no significant change in 8-week $\gamma SG^{-/-}$ muscle tissue compared with controls. However, in older mice, more profound apoptotic events may lead to significant activation of these proteins (Jung et al., 2004; Matassa et al., 2003; Trevisan et al., 2004).

Table 2. Phosphoscreen of activation in γSG$^{-/-}$ muscle relative to normal muscle

Phosphoprotein (site)	γSG$^{-/-}$ (% Normal)	Stress/stretch, mechano-transduction	Apoptosis signal	Viability signal
Hyperactivation				
(P)-ERK1(T185/Y187)	+126	Hornberger et al., 2004	Subramaniam et al., 2004; Cheung et al., 2004	
(P)-MAPKAPK2 (T222)	+114	Krook et al., 2000		
(P)-FAK (Y577)	+114	Lunn et al., 2004	Grace et al., 2003	Kurenova et al., 2004; Lin et al., 2004
(P)-MYPT1/2 (T696)	+53			
(P)-FAK (Y397)	+38	Lunn et al., 2004	Grace et al., 2003; Lesay et al., 2001	Frisch et al., 1996
No significant change in activation				
(P)-PKC-e (S729)	+16	Ni et al., 2003; Mansour et al., 2004	Jung et al., 2004	
(P)-PAX (Y31)	+10			
(P)-NR1 (S896)	+3			
(P)-Histone H3 (S28)	−2			
(P)-CREB (S133)	−3			
(P)-PKCa (S657)	−4			
(P)-PAX (Y118)	−8			
(P)-Cofilin 2 (S3)	−16			
Decreased activation				
(P)-AcCoA Carb. (S79)	−26			
(P)-Adducin-α (S662)	−40			
(P)-SMAD-1 (S463)	−40			
(P)-p38 MAPK (T180/Y182)	−54			
(P)-MAPKAP-2 (T334)	−78			
(P)-Adducin-γ (S662)	−74			

Table 3. Stretch activation of normal muscle and γSG$^{-/-}$ *

Phosphoprotein (site)	Normal (%) stretched/unstretched	γSG$^{-/-}$ (%) stretched/unstretched	Stress/stretch mechano-transduction	Apoptosis signal
Activation				
(P)-p38 MAPK (T180/Y182)	+556	+900	Martineau et al., 2001; Azuma et al., 2001; Fanning et al., 2003	Deschesnes et al., 2001
(P)-ERK1/2 (T202/Y204)	+204	+846	Jansen et al., 2004	Subramaniam et al., 2004; Cheung et al., 2004
(P)-ERK1/2 (T185/Y187)	+738	+797	Jansen et al., 2004; Hornberger et al., 2004	Subramaniam et al., 2004; Cheung et al., 2004
(P)-MAPKAPK2 (T334)	+162	+586	Krook et al., 2000; Mizutani et al., 2004	
(P)-Smad1 (S463)	−13	+39	Suzawa et al., 2002	

*After 20 minutes at ~10% stretch.

Discussion

The in vitro studies here of γSG$^{-/-}$ myotubes versus normal C57 myotubes began by extending in vivo observations of elevated apoptosis in γSG$^{-/-}$ muscle (Hack et al., 1998). A 17-fold higher apoptosis rate in vitro (at day 7, Fig. 1) may be significantly higher than the rate in vivo, but the increase could well reflect a lack of satellite cell replacement as well as other compensatory and obscuring mechanisms in vivo. The role of γSG in myotube viability appears somehow linked to moderating contractility. By several measures ranging from immunofluorescence to contractility and morphology (Figs 2-4), γSG$^{-/-}$ myotubes appear more highly prestressed or hypercontractile in vitro than normal myotubes. Moreover, although γSG is a transmembrane protein that, when absent, leads to upregulation of some membrane proteins (e.g. cortical filamin) and downregulation of others (sarcoglycans α to ε) (Hack et al., 1998; Thompson et al., 2000), γSG does not seem to contribute to adhesion (Fig. 5C). Insights into γSG-dependent signaling that might link contractility and viability as obtained in the initial screen here (Fig. 6) implicate several phosphoproteins.

Structural and functional differences suggest hypercontractility in γSG$^{-/-}$ cells

Immunofluorescence shows here that acto-myosin striations are almost twofold more frequent in γSG$^{-/-}$ myotubes than in normal myotubes (Fig. 2D). From this finding alone, these cells would be expected to be more contractile and stiffer than normal myocytes. Cells treated with contractile agonists become stiffer whereas cells in which the acto-myosin contractile apparatus is inhibited become less stiff (Hubmayr et al., 1996; Lee et al., 1998). Moreover, cell stiffness increases linearly with prestress (Wang et al., 2002).

Immunofluorescence also reveals that acto-myosin striations form only in cells-on-cells, and not in cells growing directly on the glass substrate. However, in both C57 and γSG$^{-/-}$ cells stained for actin and myosin, a majority of the collagen-coated

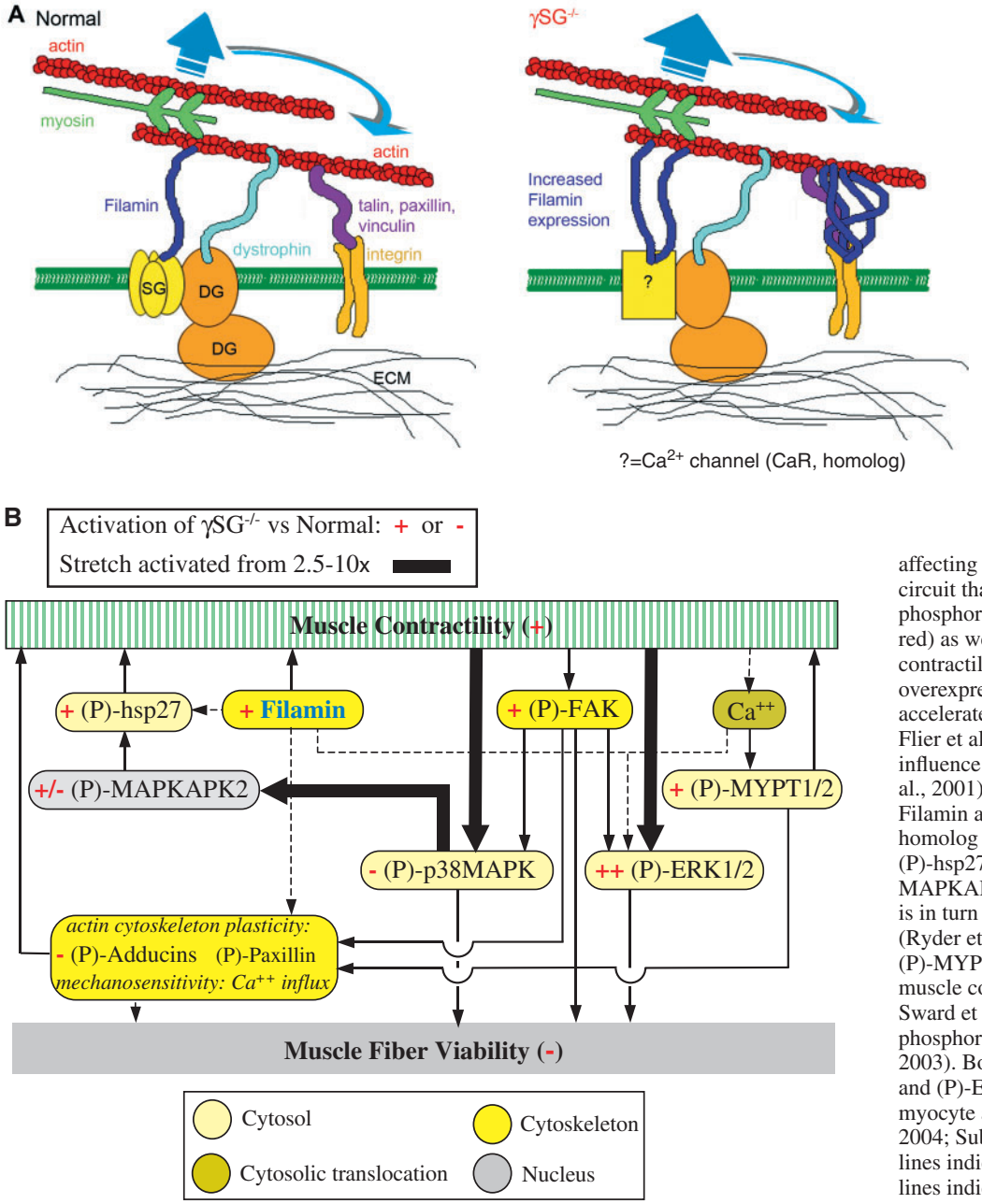

Fig. 7. Sarcoglycans and signaling. (A) Schematics of sarcolemma scaffolding in normal and γSG$^{-/-}$ muscle cells. Filamin normally associates with sarcoglycans, but in γSG$^{-/-}$ cells, sarcolemma filamin expression is considerably increased (Thompson et al., 2000). A relationship between cytoskeletal stresses and signaling via phosphorylation is posited. DG, dystroglycan; ECM, extracellular matrix; SG, sarcoglycan. The integrin adhesion complex proteins talin, paxillin, vinculin, etc., may be perturbed by the filamin over-expression, affecting signalling. (B) Proposed signaling circuit that incorporates changes in phosphorylation in γSG$^{-/-}$ tissue (+ or – in red) as well as our in vitro results for contractility and viability. Filamin-B overexpression has been shown to accelerate myotube differentiation (van der Flier et al., 2002) and is also known to influence MAP-kinase signaling (Awata et al., 2001), extending perhaps to ERK-1/2. Filamin also interacts with cvHSP, a homolog of hsp27 (Krief et al., 1999) and (P)-hsp27 is a substrate of (P)-MAPKAPK2 (Ibitayo et al., 1999), which is in turn a substrate of (P)-p38 MAPK (Ryder et al., 2000). Both (P)-hsp27 and (P)-MYPT1/2 are associated with sustained muscle contraction (Ibitayo et al., 1999; Sward et al., 2000). (P)-ERK-1/2 phosphorylates FAK (Carragher et al., 2003). Both (P)-FAK (Laprise et al., 2002) and (P)-ERK-1/2 have been linked to myocyte apoptosis (Cheung and Slack, 2004; Subramaniam et al., 2004). Dashed lines indicate proposed connections, thick lines indicate stretch-induced signals.

strips contained cells-on-cells and both upper and lower cells generally relaxed together. It is therefore safe to correlate the results of the immunofluorescent studies with the relaxing and peeling cells, noting that the overall cytoskeletal organization in γSG$^{-/-}$ cells was greater than that in C57 cells. In other words, the highly organized cytoskeleton of the upper cells drives relaxation.

This increase in cytoskeletal structure further suggests that increased prestress causes γSG$^{-/-}$ cells to relax to a greater extent than C57 cells. This is supported by the forced peeling data, which showed no difference between the two cell types, leading to the conclusion that the adhesive drag is not changed in the knockout cells. The higher prestress is also evident in the increased frequency of 'self-relaxation' with the γSG$^{-/-}$ cells. Acto-myosin contractility thus appears strong enough to break adhesive attachments of the patterned myotubes to the surface in the absence of mechanical stimulation, as evident in the high incidence of 'self-relaxation' in the γSG$^{-/-}$ cells.

Signaling possibilities for γSG

We have shown here that γSG does not factor into muscle adhesion strength; hence, γSG and the SG complex must contribute to cell function and contractility in some other way. In addition to providing a structural link between the cytoskeleton and ECM, the DGC is increasingly understood to contribute to signaling pathways (Rando, 2001). Filamin is one actin-binding protein that is widely implicated in signaling cascades that influence motility and mechanotransduction (Bellanger et al., 2000; Kainulainen et al., 2002; Leonardi et

al., 2000). This is suggestive, because although muscle-specific filamin-C binds γSG and has been reported to have a much higher level of membrane localization in γSG$^{-/-}$ tissue (Fig. 7A) (Thompson et al., 2000), overexpression of filamin-B in C2C12 cells was also recently reported to accelerate, by up to twofold, the fusion and differentiation into thin myotubes (van der Flier et al., 2002). Filamins may thus be key to the increased myotube differentiation seen here in γSG$^{-/-}$ cells. Along with the increased rate of apoptosis in γSG$^{-/-}$ myotubes found both here and by others (Hack et al., 1998), the results implicate γSG in moderating signals of differentiation and contractility that also influence viability.

Entire studies are devoted to the complex signaling cascades in muscle, and the SG-complex may be just a small, if important, component of multiple pathways. Our initial screen for possible components of relevant signaling pathways is a useful starting point, with a number of hyper- and hypophosphorylated proteins detected in C57 and γSG$^{-/-}$ muscle tissue. Combined with published results from other groups, these data lead us to propose a potential signaling pathway (Fig. 7) that would result in increased apoptosis in γSG$^{-/-}$ tissue. Thick lines indicate stretch-activated signals and dashed lines indicate likely signaling connections that have not yet been firmly documented.

First, although a signaling pathway to (P)-cJun has been connected to the DGC in rabbit skeletal muscle microsomes (Oak et al., 2003), no differences in (P)-cJun were detected here between normal C57 and γSG$^{-/-}$ tissue preparations. Of the many phosphoproteins studied, the clearest link between hypercontractility and increased apoptosis in γSG$^{-/-}$ tissue seems to be provided by the hyperactivation of ERK 1/2. In unstretched tissue, ERK1/2 was the most hyperactivated, with expression in γSG$^{-/-}$ tissue 126% greater than that in normal tissue (Table 2). This is particularly interesting given the role of (P)-ERK in mechanotransduction, sarcomeric reorganization, and as a regulator of apoptosis (Hornberger et al., 2005; Kumar et al., 2004; Loth et al., 2003; Ryder et al., 2000; Zechner et al., 1997). Moreover, Kumar and colleagues recently demonstrated with ex vivo muscle fibers that ERK1/2 is activated by externally imposed stretch (Kumar et al., 2002), data confirmed by our phosphoscreens (Table 3). Importantly, ERK 1/2 phosphorylation increased by more than 800% in stretched γSG$^{-/-}$ tissue compared with unstretched, but activity in stretched normal tissue increased by only 200%. ERK 1/2 activation has previously been linked to increased apoptosis (Cheung et al., 2004; Subramaniam et al., 2004), so the overstretched or hypercontractile character of adherent γSG$^{-/-}$ cells in vitro (Figs 3-4) may provide the extra stimulus towards apoptosis via a (P)-ERK 1/2 pathway (Fig. 7), which may translate to γSG$^{-/-}$ tissue in vivo.

MAPKAPK2 is also hyperactivated, with 114% activation in γSG$^{-/-}$ muscle tissue compared with normal muscle (Table 2). MAPKAPK2 has been shown to stimulate muscle contractility via (P)-hsp27 (Ibitayo et al., 1999), which also appears to be activated in γSG$^{-/-}$ tissue but not in C57 tissue. Because (P)-MAPKAPK2 is a target for (P)-ERK and is itself stretch-activated (Ibitayo et al., 1999; Krook et al., 2000; Mizutani et al., 2004; Ryder et al., 2000), these proteins may be part of a hypercontractile signaling loop (Fig. 7) that couples to externally imposed (stretch) as well as internally generated mechanical stress (prestress). However, the function may depend on site-specific phosphorylation. Consistent with hypercontractility, the myosin phosphatase MYPT1/2 also appeared more phosphorylated in γSG$^{-/-}$ tissue than in C57 tissue. It has recently been shown that phosphorylation of MYPT inhibits myosin light chain phosphatase activity, leading to increased myosin phosphorylation and higher force (Sward et al., 2000). MYPT1/2 probably sits in a parallel signaling pathway coupled to intracellular calcium levels, which are altered in dystrophin-depleted murine tissue (Fong et al., 1990).

Another link between hypercontractility and increased apoptosis in γSG$^{-/-}$ tissue is provided by increased activation in stretched γSG$^{-/-}$ tissue of p38 MAPK and MAPKAP2 in addition to ERK. P38 MAPK is known to be stretch- and stress-activated (Azuma et al., 2001; Martineau and Gardiner, 2001; Mizutani et al., 2004), and increased phosphorylation of p38 MAPK has been linked to increased apoptosis (Deschesnes et al., 2001). Thus, although we found that p38 MAPK exhibits decreased activation in unstretched γSG$^{-/-}$ tissue (Table 2), the 900% increase of p38 MAPK phosphorylation in stretched γSG$^{-/-}$ tissue (compared with a 500% increase in stretched normal cells) (Table 3) reveals its sensitivity to mechanotransduction. It should be noted that while overall phosphoprotein levels after 20 minutes at ~10% stretch happen to be similar to normal C57 tissue after similar length change and time, MAPK activation is known to be a quantitative reflection of the magnitude of mechanical stress applied to muscle (Martineau and Gardiner, 2001), and so longer times and larger stretches are likely to be different, especially given the large changes here. More thorough investigations are certainly needed. In light of the sensitive response of p38 MAPK to stretching in both normal and γSG$^{-/-}$ tissue, we suggest that the hypercontractility of the γSG$^{-/-}$ cells in vitro may also trigger a p38 MAPK apoptotic signaling cascade (Fig. 7),

We have further investigated a possible cross-talk between p38 MAPK and MAPKAP2 and a role for heat shock protein 27 (hsp27) in mediating this interaction under externally imposed stress (stretch) in normal and γSG$^{-/-}$ muscle (Fig. 7). In parallel, these midstream mediators can interact with molecules of other signaling pathways. Here we suggest that ERK1/2 and FAK signal the survival/apoptotic pathway (Cheung and Slack, 2004; Frisch et al., 1996). (P)-ERK has been shown to phosphorylate FAK (Carragher et al., 2003), and we found (P)-FAK/Y397 and Y577 are hyperactivated in γSG$^{-/-}$ tissue. FAK is believed to associate with the DGC through the signaling protein Grb2 (Cavaldesi et al., 1999). Both (P)-FAK and (P)-ERK have also been associated with myocyte apoptosis (Cheung and Slack, 2004; Kurenova et al., 2004; Lin et al., 2004; Liu and Hofmann, 2004; Subramaniam et al., 2004). The balance between ERK and JNK/p38 MAPK is critical in signaling apoptosis or viability (Xia et al., 1995). A recent study has revealed that ERK is a key apoptotic factor in potassium deprivation-induced neuronal cell death by showing that ERK inhibitors protect neurons from low potassium conditions, whereas constitutively activated ERK activates cell death. Most importantly, this study shows how ERK can promote neuronal cell death by causing plasma membrane and DNA damage that is independent of caspase-3 activity (Subramaniam et al., 2004). Further studies on the mechanism of ERK in neuronal cell death may shed light on

the possibility of using ERK as a therapeutic target in treating neurodegeneration.

Structural targets also showed differential phosphorylation: adducin was found to be less phosphorylated in γSG$^{-/-}$ muscle and is well known to associate with actin and thus influence cytoskeletal organization (Matsuoka et al., 2000). Coupled to the hypercontractile state of γSG$^{-/-}$ cells, a different cytoskeletal organization in these cells is consistent with our findings (Fig. 2). (P)-adducin-α has also been linked to apoptosis in epithelial cells (Imamdi et al., 2004; van de Water et al., 2000), and has been suggested as a monitor of ERK1/2 activity (Je et al., 2004). Downregulation of activated adducin could thus play a part in the runaway activation of ERK1/2 in γSG$^{-/-}$ tissue.

Beyond the scope of this initial phosphoscreen where we have primarily focused on the upstream and midstream mediators of apoptosis and myocyte mechanics, further studies would help clarify the signaling cascade that has gone awry in γSG$^{-/-}$ cells. Several, sensible candidates like p38 MAPK, MAPKAP2 and Smad1 for deeper examination of protein interactions have been identified in stretch-induced mechanotransduction. The phosphoscreen results corroborate our in vitro studies as well as the data of other groups on increased apoptosis in γSG$^{-/-}$ cells. Activation of the MAPK pathways in γSG$^{-/-}$ cells begins to establish a signaling link to apoptosis (Cheung and Slack, 2004; Lesay et al., 2001; Xia et al., 1995). Given the lack of adhesive defect in these cells, as some of the adhesion proteins like paxillin remain unchanged, it is becoming increasingly clear that molecular signaling is critical in the progression of limb girdle muscular dystrophy (LGMD2C). Future studies might not only clarify the coupled signaling circuits but also eventually lead to pharmacological interventions.

In summary, we have shown that myotubes lacking γSG have an acto-myosin cytoskeleton that is more organized than that of normal myotubes, at least when growing on top of other compliant cells. This organization increases the overall cellular prestress. Future studies involving contractile agonists and/or antagonists could serve to elucidate the contribution of the acto-myosin network to the prestress of skeletal myotubes. In addition, apoptosis is increased in γSG$^{-/-}$ cells in vitro, corroborating previous tissue-level studies by another group (Hack et al., 1998). We propose that γSG is part of a signaling cascade, which controls the rate of sarcomerogenesis and/or apoptosis. Specifically, activation of ERK, p38 MAPK and MAPKAP2 as well as FAK phosphoproteins indicates that distinct MAPK signaling pathways contribute to contractile stress and high occurrence of apoptosis in the muscular dystrophy phenotype expressed by mice and humans lacking the gene for γSG.

We gratefully acknowledge Elizabeth N. McNally for the γSG$^{-/-}$ mice and for very useful discussions. We would also like to thank Shamik Sen and Adam Engler for help in maintaining cell cultures, and Elisabeth Barton for helpful discussion. This work was funded by the NIH and the MDA.

References

Awata, H., Huang, C., Handlogten, M. E. and Miller, R. T. (2001). Interaction of the calcium-sensing receptor and filamin, a potential scaffolding protein. *J. Biol. Chem.* **276**, 34871-34879.

Azuma, N., Akasaka, N., Kito, H., Ikeda, M., Gahtan, V., Sasajima, T. and Sumpio, B. E. (2001). Role of p38 MAP kinase in endothelial cell alignment induced by fluid shear stress. *Am. J. Physiol. Heart Circ. Physiol.* **280**, H189-H197.

Bellanger, J. M., Astier, C., Sardet, C., Ohta, Y., Stossel, T. P. and Debant, A. (2000). The Rac1- and RhoG-specific GEF domain of Trio targets filamin to remodel cytoskeletal actin. *Nat. Cell Biol.* **2**, 888-892.

Bradley, W. G. and Fulthorpe, J. J. (1978). Studies of sarcolemmal integrity in myopathic muscle. *Neurology* **28**, 670-677.

Bushby, K. M. (1999). The limb-girdle muscular dystrophies-multiple genes, multiple mechanisms. *Hum. Mol. Genet.* **8**, 1875-1882.

Carragher, N. O., Westhoff, M. A., Fincham, V. J., Schaller, M. D. and Frame, M. C. (2003). A novel role for FAK as a protease-targeting adaptor protein: regulation by p42 ERK and Src. *Curr. Biol.* **13**, 1442-1450.

Cavaldesi, M., Macchia, G., Barca, S., Defilippi, P., Tarone, G. and Petrucci, T. C. (1999). Association of the dystroglycan complex isolated from bovine brain synaptosomes with proteins involved in signal transduction. *J. Neurochem.* **72**, 1648-1655.

Cheung, E. C. and Slack, R. S. (2004). Emerging role for ERK as a key regulator of neuronal apoptosis. *Sci. STKE* **2004**, PE45.

Deschesnes, R. G., Huot, J., Valerie, K. and Landry, J. (2001). Involvement of p38 in apoptosis-associated membrane blebbing and nuclear condensation. *Mol. Biol. Cell* **12**, 1569-1582.

Engler, A., Bacakova, L., Newman, C., Hategan, A., Griffin, M. and Discher, D. (2004a). Substrate compliance versus ligand density in cell on gel responses. *Biophys. J.* **86**, 617-628.

Engler, A. J., Griffin, M. A., Sen, S., Bonnemann, C. G., Sweeney, H. L. and Discher, D. E. (2004b). Myotubes differentiate optimally on substrates with tissue-like stiffness: pathological implications for soft or stiff microenvironments. *J. Cell Biol.* **166**, 877-887.

Fanning, P. J., Emkey, G., Smith, R. J., Grodzinsky, A. J., Szasz, N. and Trippel, S. B. (2003). Mechanical regulation of mitogen-activated protein kinase signaling in articular cartilage. *J. Biol. Chem.* **278**, 50940-50948.

Fong, P. Y., Turner, P. R., Denetclaw, W. F. and Steinhardt, R. A. (1990). Increased activity of calcium leak channels in myotubes of Duchenne human and mdx mouse origin. *Science* **250**, 673-676.

Frisch, S. M., Vuori, K., Ruoslahti, E. and Chan-Hui, P. Y. (1996). Control of adhesion-dependent cell survival by focal adhesion kinase. *J. Cell Biol.* **134**, 793-799.

Grace, E. A. and Busciglio, J. (2003). Aberrant activation of focal adhesion proteins mediates fibrillar amyloid beta-induced neuronal dystrophy. *J. Neurosci.* **23**, 493-502.

Grady, R. M., Merlie, J. P. and Sanes, J. R. (1997). Subtle neuromuscular defects in utrophin-deficient mice. *J. Cell Biol.* **136**, 871-882.

Griffin, M. A., Engler, A. J., Barber, T. A., Healy, K. E., Sweeney, H. L. and Discher, D. E. (2004a). Patterning, prestress, and peeling dynamics of myocytes. *Biophys. J.* **86**, 1209-1222.

Griffin, M. A., Sen, S., Sweeney, H. L. and Discher, D. E. (2004b). Adhesion-contractile balance in myocyte differentiation. *J. Cell Sci.* **117**, 5855-5863.

Hack, A. A., Cordier, L., Shoturma, D. I., Lam, M. Y., Sweeney, H. L. and McNally, E. M. (1999). Muscle degeneration without mechanical injury in sarcoglycan deficiency. *Proc. Natl. Acad. Sci. USA* **96**, 10723-10728.

Hack, A. A., Ly, C. T., Jiang, F., Clendenin, C. J., Sigrist, K. S., Wollmann, R. L. and McNally, E. M. (1998). Gamma-sarcoglycan deficiency leads to muscle membrane defects and apoptosis independent of dystrophin. *J. Cell Biol.* **142**, 1279-1287.

Hornberger, T. A., Armstrong, D. D., Koh, T. J., Burkholder, T. J. and Esser, K. A. (2005). Intracellular signaling specificity in response to uniaxial vs. multiaxial stretch: implications for mechanotransduction. *Am. J. Physiol. Cell Physiol.* **288**, C185-C194.

Hubmayr, R. D., Shore, S. A., Fredberg, J. J., Planus, E., Panettieri, R. A., Jr, Moller, W., Heyder, J. and Wang, N. (1996). Pharmacological activation changes stiffness of cultured human airway smooth muscle cells. *Am. J. Physiol.* **271**, C1660-C1668.

Ibitayo, A. I., Sladick, J., Tuteja, S., Louis-Jacques, O., Yamada, H., Groblewski, G., Welsh, M. and Bitar, K. N. (1999). HSP27 in signal transduction and association with contractile proteins in smooth muscle cells. *Am. J. Physiol.* **277**, G445-G454.

Imamdi, R., de Graauw, M. and van de Water, B. (2004). Protein kinase C mediates cisplatin-induced loss of adherens junctions followed by apoptosis of renal proximal tubular epithelial cells. *J. Pharmacol. Exp. Ther.* **311**, 892-903.

Jansen, J. H., Weyts, F. A., Westbroek, I., Jahr, H., Chiba, H., Pols, H. A.,

Verhaar, J. A., van Leeuwen, J. P. and Weinans, H. (2004). Stretch-induced phosphorylation of ERK1/2 depends on differentiation stage of osteoblasts. *J. Cell. Biochem.* **93**, 542-551.
Je, H. D., Gallant, C., Leavis, P. C. and Morgan, K. G. (2004). Caveolin-1 regulates contractility in differentiated vascular smooth muscle. *Am. J. Physiol. Heart Circ. Physiol.* **286**, H91-H98.
Jung, Y. S., Ryu, B. R., Lee, B. K., Mook-Jung, I., Kim, S. U., Lee, S. H., Baik, E. J. and Moon, C. H. (2004). Role for PKC-epsilon in neuronal death induced by oxidative stress. *Biochem. Biophys. Res. Commun.* **320**, 789-794.
Kaariainen, M., Kaariainen, J., Jarvinen, T. L., Nissinen, L., Heino, J., Jarvinen, M. and Kalimo, H. (2000). Integrin and dystrophin associated adhesion protein complexes during regeneration of shearing-type muscle injury. *Neuromuscul. Disord.* **10**, 121-132.
Kainulainen, T., Pender, A., D'Addario, M., Feng, Y., Lekic, P. and McCulloch, C. A. (2002). Cell death and mechanoprotection by filamin a in connective tissues after challenge by applied tensile forces. *J. Biol. Chem.* **277**, 21998-22009.
Kramarcy, N. R. and Sealock, R. (1990). Dystrophin as a focal adhesion protein. Collocalization with talin and the Mr 48,000 sarcolemmal protein in cultured Xenopus muscle. *FEBS Lett.* **274**, 171-174.
Krief, S., Faivre, J. F., Robert, P., le Douarin, B., Brument-Larignon, N., Lefrere, I., Bouzyk, M. M., Anderson, K. M., Greller, L. D., Tobin, F. L. et al. (1999). Identification and characterization of cvHsp. A novel human small stress protein selectively expressed in cardiovascular and insulin-sensitive tissues. *J. Biol. Chem.* **274**, 36592-36600.
Krook, A., Widegren, U., Jiang, X. J., Henriksson, J., Wallberg-Henriksson, H., Alessi, D. and Zierath, J. R. (2000). Effects of exercise on mitogen- and stress-activated kinase signal transduction in human skeletal muscle. *Am. J. Physiol. Regul. Integr. Comp. Physiol.* **279**, R1716-R1721.
Kumar, A., Chaudhry, I., Reid, M. B. and Boriek, A. M. (2002). Distinct signaling pathways are activated in response to mechanical stress applied axially and transversely to skeletal muscle fibers. *J. Biol. Chem.* **277**, 46493-46503.
Kumar, A., Khandelwal, N., Malya, R., Reid, M. B. and Boriek, A. M. (2004). Loss of dystrophin causes aberrant mechanotransduction in skeletal muscle fibers. *FASEB J.* **18**, 102-113.
Kurenova, E., Xu, L. H., Yang, X., Baldwin, A. S., Jr, Craven, R. J., Hanks, S. K., Liu, Z. G. and Cance, W. G. (2004). Focal adhesion kinase suppresses apoptosis by binding to the death domain of receptor-interacting protein. *Mol. Cell. Biol.* **24**, 4361-4371.
Lakonishok, M., Muschler, J. and Horwitz, A. F. (1992). The alpha 5 beta 1 integrin associates with a dystrophin-containing lattice during muscle development. *Dev. Biol.* **152**, 209-220.
Laprise, P., Poirier, E. M., Vezina, A., Rivard, N. and Vachon, P. H. (2002). Merosin-integrin promotion of skeletal myofiber cell survival: Differentiation state-distinct involvement of p60Fyn tyrosine kinase and p38alpha stress-activated MAP kinase. *J. Cell Physiol.* **191**, 69-81.
Lee, K. M., Tsai, K. Y., Wang, N. and Ingber, D. E. (1998). Extracellular matrix and pulmonary hypertension: control of vascular smooth muscle cell contractility. *Am. J. Physiol.* **274**, H76-H82.
Leonardi, A., Ellinger-Ziegelbauer, H., Franzoso, G., Brown, K. and Siebenlist, U. (2000). Physical and functional interaction of filamin (actin-binding protein-280) and tumor necrosis factor receptor-associated factor 2. *J. Biol. Chem.* **275**, 271-278.
Lesay, A., Hickman, J. A. and Gibson, R. M. (2001). Disruption of focal adhesions mediates detachment during neuronal apoptosis. *Neuroreport* **12**, 2111-2115.
Lin, E. H., Hui, A. Y., Meens, J. A., Tremblay, E. A., Schaefer, E. and Elliott, B. E. (2004). Disruption of Ca2+-dependent cell-matrix adhesion enhances c-Src kinase activity, but causes dissociation of the c-Src/FAK complex and dephosphorylation of tyrosine-577 of FAK in carcinoma cells. *Exp. Cell Res.* **293**, 1-13.
Liu, Q. and Hofmann, P. A. (2004). Protein phosphatase 2A-mediated cross-talk between p38 MAPK and ERK in apoptosis of cardiac myocytes. *Am. J. Physiol. Heart Circ. Physiol.* **286**, H2204-H2212.
Loth, F., Fischer, P. F., Arslan, N., Bertram, C. D., Lee, S. E., Royston, T. J., Shaalan, W. E. and Bassiouny, H. S. (2003). Transitional flow at the venous anastomosis of an arteriovenous graft: potential activation of the ERK1/2 mechanotransduction pathway. *J. Biomech. Eng.* **125**, 49-61.
Lunn, J. A. and Rozengurt, E. (2004). Hyperosmotic stress induces rapid focal adhesion kinase phosphorylation at tyrosines 397 and 577. Role of Src family kinases and Rho family GTPases. *J. Biol. Chem.* **279**, 45266-45278.
Mansour, H., de Tombe, P. P., Samarel, A. M. and Russell, B. (2004). Restoration of resting sarcomere length after uniaxial static strain is regulated by protein kinase Cepsilon and focal adhesion kinase. *Circ. Res.* **94**, 642-649.
Martineau, L. C. and Gardiner, P. F. (2001). Insight into skeletal muscle mechanotransduction: MAPK activation is quantitatively related to tension. *J. Appl. Physiol.* **91**, 693-702.
Matassa, A. A., Kalkofen, R. L., Carpenter, L., Biden, T. J. and Reyland, M. E. (2003). Inhibition of PKCalpha induces a PKCdelta-dependent apoptotic program in salivary epithelial cells. *Cell Death Differ.* **10**, 269-277.
Matsuoka, Y., Li, X. and Bennett, V. (2000). Adducin: structure, function and regulation. *Cell. Mol. Life Sci.* **57**, 884-895.
Mizutani, T., Fukushi, S., Saijo, M., Kurane, I. and Morikawa, S. (2004). Phosphorylation of p38 MAPK and its downstream targets in SARS coronavirus-infected cells. *Biochem. Biophys. Res. Commun.* **319**, 1228-1234.
Neville, C., Rosenthal, N., McGraw, M., Bogdanova, N. and Hauschka, S. D. (1998). *Skeletal muscle cultures*. San Diego, CA: Academic Press.
Ni, C. W., Wang, D. L., Lien, S. C., Cheng, J. J., Chao, Y. J. and Hsieh, H. J. (2003). Activation of PKC-epsilon and ERK1/2 participates in shear-induced endothelial MCP-1 expression that is repressed by nitric oxide. *J. Cell. Physiol.* **195**, 428-434.
Noguchi, S., McNally, E. M., Ben Othmane, K., Hagiwara, Y., Mizuno, Y., Yoshida, M., Yamamoto, H., Bonnemann, C. G., Gussoni, E., Denton, P. H. et al. (1995). Mutations in the dystrophin-associated protein gamma-sarcoglycan in chromosome 13 muscular dystrophy. *Science* **270**, 819-822.
Oak, S. A., Zhou, Y. W. and Jarrett, H. W. (2003). Skeletal muscle signaling pathway through the dystrophin glycoprotein complex and Rac1. *J. Biol. Chem.* **278**, 39287-39295.
Paul, A. C., Sheard, P. W., Kaufman, S. J. and Duxson, M. J. (2002). Localization of alpha 7 integrins and dystrophin suggests potential for both lateral and longitudinal transmission of tension in large mammalian muscles. *Cell Tissue Res.* **308**, 255-265.
Pelech, S., Sutter, C. and Zhang, H. (2003). Kinetworks™ Protein Kinase Multiblot Analysis. In *Cancer Cell Signaling: Methods and Protocols*, vol. 218 (ed. D. M. Terrian), pp. 99-111. Totowa, N.J.: Humana Press.
Potard, U. S., Butler, J. P. and Wang, N. (1997). Cytoskeletal mechanics in confluent epithelial cells probed through integrins and E-cadherins. *Am. J. Physiol.* **272**, C1654-C1663.
Radojevic, V., Lin, S. and Burgunder, J. M. (2000). Differential expression of dystrophin, utrophin, and dystrophin-associated proteins in human muscle culture. *Cell Tissue Res.* **300**, 447-457.
Rando, T. A. (2001). The dystrophin-glycoprotein complex, cellular signaling, and the regulation of cell survival in the muscular dystrophies. *Muscle Nerve* **24**, 1575-1594.
Ryder, J. W., Fahlman, R., Wallberg-Henriksson, H., Alessi, D. R., Krook, A. and Zierath, J. R. (2000). Effect of contraction on mitogen-activated protein kinase signal transduction in skeletal muscle. Involvement Of the mitogen- and stress-activated protein kinase 1. *J. Biol. Chem.* **275**, 1457-1462.
Scherer, A. and Graff, J. M. (2000). Calmodulin differentially modulates Smad1 and Smad2 signaling. *J. Biol. Chem.* **275**, 41430-41438.
Stamenovic, D., Liang, Z., Chen, J. and Wang, N. (2002). Effect of the cytoskeletal prestress on the mechanical impedance of cultured airway smooth muscle cells. *J. Appl. Physiol.* **92**, 1443-1450.
Straub, V., Rafael, J. A., Chamberlain, J. S. and Campbell, K. P. (1997). Animal models for muscular dystrophy show different patterns of sarcolemmal disruption. *J. Cell Biol.* **139**, 375-385.
Subramaniam, S., Zirrgiebel, U., von Bohlen Und Halbach, O., Strelau, J., Laliberte, C., Kaplan, D. R. and Unsicker, K. (2004). ERK activation promotes neuronal degeneration predominantly through plasma membrane damage and independently of caspase-3. *J. Cell Biol.* **165**, 357-369.
Suzawa, M., Tamura, Y., Fukumoto, S., Miyazono, K., Fujita, T., Kato, S. and Takeuchi, Y. (2002). Stimulation of Smad1 transcriptional activity by Ras-extracellular signal-regulated kinase pathway: a possible mechanism for collagen-dependent osteoblastic differentiation. *J. Bone Miner. Res.* **17**, 240-248.
Sward, K., Dreja, K., Susnjar, M., Hellstrand, P., Hartshorne, D. J. and Walsh, M. P. (2000). Inhibition of Rho-associated kinase blocks agonist-induced Ca2+ sensitization of myosin phosphorylation and force in guinea-pig ileum. *J. Physiol.* **522**, 33-49.
Thompson, T. G., Chan, Y. M., Hack, A. A., Brosius, M., Rajala, M., Lidov,

H. G., McNally, E. M., Watkins, S. and Kunkel, L. M. (2000). Filamin 2 (FLN2): A muscle-specific sarcoglycan interacting protein. *J. Cell Biol.* **148**, 115-126.

Trevisan, R., Daprai, L., Acquasaliente, L., Ciminale, V., Chieco-Bianchi, L. and Saggioro, D. (2004). Relevance of CREB phosphorylation in the anti-apoptotic function of human T-lymphotropic virus type 1 tax protein in serum-deprived murine fibroblasts. *Exp. Cell Res.* **299**, 57-67.

van de Water, B., Tijdens, I. B., Verbrugge, A., Huigsloot, M., Dihal, A. A., Stevens, J. L., Jaken, S. and Mulder, G. J. (2000). Cleavage of the actin-capping protein alpha-adducin at Asp-Asp-Ser-Asp633-Ala by caspase-3 is preceded by its phosphorylation on serine 726 in cisplatin-induced apoptosis of renal epithelial cells. *J. Biol. Chem.* **275**, 25805-25813.

van der Flier, A., Kuikman, I., Kramer, D., Geerts, D., Kreft, M., Takafuta, T., Shapiro, S. S. and Sonnenberg, A. (2002). Different splice variants of filamin-B affect myogenesis, subcellular distribution, and determine binding to integrin [beta] subunits. *J. Cell Biol.* **156**, 361-376.

Wang, N., Butler, J. P. and Ingber, D. E. (1993). Mechanotransduction across the cell surface and through the cytoskeleton. *Science* **260**, 1124-1127.

Wang, N., Tolic-Norrelykke, I. M., Chen, J., Mijailovich, S. M., Butler, J. P., Fredberg, J. J. and Stamenovic, D. (2002). Cell prestress. I. Stiffness and prestress are closely associated in adherent contractile cells. *Am. J. Physiol. Cell Physiol.* **282**, C606-C616.

Xia, Z., Dickens, M., Raingeaud, J., Davis, R. J. and Greenberg, M. E. (1995). Opposing effects of ERK and JNK-p38 MAP kinases on apoptosis. *Science* **270**, 1326-1331.

Yoshida, T., Hanada, H., Iwata, Y., Pan, Y. and Sigekawa, M. (1996). Expression of a dystrophin-sarcoglycan complex in serum-deprived BC3H1 cells and involvement of alpha-sarcoglycan in substrate attachment. *Biochem. Biophys. Res. Commun.* **225**, 11-15.

Yoshida, T., Pan, Y., Hanada, H., Iwata, Y. and Shigekawa, M. (1998). Bidirectional signaling between sarcoglycans and the integrin adhesion system in cultured L6 myocytes. *J. Biol. Chem.* **273**, 1583-1590.

Zechner, D., Thuerauf, D. J., Hanford, D. S., McDonough, P. M. and Glembotski, C. C. (1997). A role for the p38 mitogen-activated protein kinase pathway in myocardial cell growth, sarcomeric organization, and cardiac-specific gene expression. *J. Cell Biol.* **139**, 115-127.